Turkish Journal of Electrical Engineering & Computer Sciences

http://journals.tubitak.gov.tr/elektrik/

Research Article

Turk J Elec Eng & Comp Sci
(2015) 23: 1230 – 1241

doi:10.3906/elk-1301-203

Regulation of methane gas output from an anaerobic reactor system using moving horizon $\mathcal{H}_\infty$ control

Fatma YILDIZ TAŞCIKARAOĞLU, Şeref Naci ENGİN*
Control and Automation Engineering Department, Yıldız Technical University, Istanbul, Turkey

Received: 28.01.2013 • **Accepted/Published Online:** 05.03.2013 • **Printed:** 28.08.2015

Abstract: In this study, the moving horizon $\mathcal{H}_\infty$ control used for tracking a desired methane gas output from an anaerobic wastewater treatment reactor is compared with classical $\mathcal{H}_\infty$ control and a proportional-integral-derivative controller. The nonlinear system is first linearized around the set of equilibrium and operating points selected, and then the linear matrix inequalities required to comply with the constraints and guarantee the stability are constructed. Finally, the experimental results are obtained by implementing the control method in a MATLAB environment. It is concluded that moving horizon $\mathcal{H}_\infty$ control yields satisfactory results.

Key words: Anaerobic reactor system, moving horizon $\mathcal{H}_\infty$ control, linear matrix inequality

1. Introduction

In this paper, moving horizon control (MHC), which has found quite a large area of application, is taken into consideration in order to guarantee the $\mathcal{H}_\infty$ performance of a nonlinear process containing input and output constraints in the case where a constrained disturbance is in effect. The work by Mayne et al. [1] can be listed as one of the most significant studies reporting the development of MHC, which is also referred to as model predictive control (MPC) or receding horizon control. On the other hand, the study by Qin and Badgwell [2], which examines the practical features of the method, has been cited many times. It was comprehensively studied in the literature from the theoretical points of view as a Riccati-based controller [3,4] and linear matrix inequality (LMI)-based controller [5–9]. Its practical applications can be found commonly in chemical and environmental processes [10,11].

Inadequately treated wastewater discharge from point sources to receiving media leads to serious environmental problems. Efficient and cost-effective treatment methods are, therefore, needed for the protection of water resources. Anaerobic treatment is considered as a proven and energy efficient method to treat industrial wastewaters having high organic matter content. Anaerobic treatment has many advantages over aerobic treatment from the viewpoint of low energy use, small footprint, and low sludge production. Furthermore, a high value-added product, namely biogas, is produced during the conversion of organic matter into final products. Anaerobic digestion is a 3-stage process involving hydrolysis, acidogenesis/acetogenesis, and methanogenesis phases, which depend on the synergistic relationship of the bacterial consortia present in the reactor. Therefore, control of such a complex biological system is quite an important task. A number of different control methodologies have been developed and employed in recent years.

*Correspondence: nengin@yildiz.edu.tr

In MPC, the mathematical model of the system to be controlled is used to predict the future behavior of the plant. The ratio between the norms of disturbance and the controlled output, which is the difference between the reference input and the predicted output, is minimized with the solution of the online $\mathcal{H}_\infty$ optimal control along a prediction horizon within the input and output constraints, [12]. The classical $\mathcal{H}_\infty$ problem is solved recursively at each step k under the input and output constraints, guaranteeing the dissipation for the case where a linear discrete model is considered. In order to optimize the trade-off between the performance requirements and control constraints, $\mathcal{H}_\infty$ control has been widely utilized in the literature of optimal control. LMIs taken from [7,8] are used for the solution of the $\mathcal{H}_\infty$ control problem within the frame of MPC.

In this work, an anaerobic wastewater treatment model is taken into consideration, where a linearization procedure is carried out around the set of equilibrium points and an attempt is made to maintain the methane (CH_4) gas output at a desired level while adopting the moving horizon $\mathcal{H}_\infty$ control. This paper is organized as follows. A nonlinear mathematical model describing the anaerobic reactor system with which the regulation of CH_4 gas is to be carried out is presented in Section 2. By means of linearizing this model around the set of equilibrium points, a linear state-space model of the system is obtained and presented in Section 3. Section 3 also describes the state feedback control system with an observer, which is designed to estimate the unmeasurable states from the measured output and the input introduced. The moving horizon $\mathcal{H}_\infty$ control algorithm and derivation of the LMIs used in this algorithm are presented in Section 4. In Section 5, the control method adopted together with the classical $\mathcal{H}_\infty$ and a proportional-integral-derivative (PID) controller is applied to the anaerobic system of interest, and the regulation results are presented with plots. The work accomplished is briefly summarized and the conclusions derived from the method proposed for the control of the anaerobic system are presented in Section 6.

2. Anaerobic system

Anaerobic treatment requires careful monitoring and control systems, as these systems are quite sensitive due to their intrinsic complexity. For this reason, advanced control techniques are applied to these bioprocesses in order to fulfill the requirements. A model of an anaerobic treatment process is considered on the basis of 4 succeeding reactions, namely hydrolysis, acidogenesis, acetogenesis, and methanogenesis. The organic substrate present in the wastewater is degraded into volatile fatty acids (VFAs) by acidogenic and acetogenic bacteria after hydrolysis, and, as a succeeding step, the VFAs are degraded into CH_4, carbon dioxide (CO_2), and some other gases by methanogenic bacteria. The mathematical model of a 2-stage continuously stirred tank bioreactor is described by the following ordinary differential equations:

$$\begin{aligned}
\frac{dX_1}{dt} &= (\mu_1 - D)\, X_1 \\
\frac{dX_2}{dt} &= (\mu_2 - D)\, X_2 \\
\frac{dS_1}{dt} &= D\left(S_1^{in} - S_1\right) X_1 - \mu_1\, k_1 X_1 \\
\frac{dS_2}{dt} &= D\,(S_1 - S_2) + \mu_1\, k_2 X_1 - \mu_2 k_3 X_2
\end{aligned} \tag{1}$$

Here, the state variables of the system, X_1 and X_2, denote the biomass concentrations and S_1 and S_2 denote the substrate concentrations. The disturbance, which is the influent concentration, is denoted by S_1^{in}. The

dilution rate (D) is chosen as the control input. The specific growth rate of the microorganism's μ is defined as given in Eq. (2).

$$\mu = \frac{\mu_{\max} + S}{K_S + S} \tag{2}$$

Here, $K_s k_1 k_2 k_3$ are the coefficients. The methane flow rate is the measurable output and is denoted by Q, as shown in Eq. (3).

$$Q = k_4 \mu_2 X_2 \tag{3}$$

3. System linearization

The system given in Eq. (1) can be represented by the following differential equation.

$$\dot{x}(t) = f(x(t), w(t), u(t)) \tag{4}$$

The state vector $x(t)$, disturbance $w(t)$, and control input $u(t)$ are defined as:

$$x(t) = \begin{bmatrix} X_1(t) \\ X_2(t) \\ S_1(t) \\ S_2(t) \end{bmatrix}, \quad w(t) = \left[S_1^{in}(t)\right], \quad u(t) = [D(t)] \tag{5}$$

The nonlinear system linearized using the Jacobian linearization technique at the equilibrium point of the corresponding states is given by:

$$\left[\frac{dX_1}{dt}, \frac{dX_2}{dt}, \frac{dS_1}{dt}, \frac{dS_2}{dt}\right] = [0, 0, 0, 0] \tag{6}$$

The steady-state values of $X_1^* X_2^* S_1^* S_2^*$ then become:

$$S_1^* = K_{S1}\frac{D}{\mu_{max1} - D} \quad S_2^* = K_{S2}\frac{D}{\mu_{max2} - D}$$
$$X_1^* = \frac{1}{K_1}\left(S_1^{in} - S_1^*\right) \quad X_2^* = \frac{1}{K_3}\left[(S_1^* - S_2^*) + \frac{K_2}{K_1}\left(S_1^{in} - S_1^*\right)\right] \tag{7}$$

According to the steady-state values given, the Jacobian linearization of the nonlinear system can be given as follows:

$$\dot{\delta_x}(t) = A\delta_x(t) + B_w\delta_w(t) + B_u\delta_u(t) \tag{8}$$

where the deviation variables are defined as:

$$\delta_x(t) = x(t) - x^*$$
$$\delta_w(t) = w(t) - w^* \tag{9}$$
$$\delta_u(t) = u(t) - u^*$$

and the matrices composed of the partial derivatives are defined as:

$$A = \frac{df}{dx}\Big|_{x^*,w^*,u^*} \in R^{4x4}, \quad B_w = \frac{df}{dw}\Big|_{x^*,w^*,u^*} \in R^{4x1}, \quad B_u = \frac{df}{du}\Big|_{x^*,w^*,u^*} \in R^{4x1} \tag{10}$$

Utilizing the steady-state values denoted in Eq. (7), the matrices are obtained as follows:

$$A = \begin{bmatrix} \mu_1^* - D^* & 0 & a_1 X_1^* & 0 \\ 0 & \mu_2^* - D^* & 0 & a_2 X_2^* \\ -\mu_1^* k_1 & 0 & -D - a_1 k_1 X_1^* & 0 \\ \mu_1^* k_2 & -\mu_2^* k_3 & D + a_1 k_2 X_1^* & -D^* - a_2 k_3 X_2^* \end{bmatrix} \tag{11}$$

where

$$a_1 = \frac{\mu_{1max}^* K_{S1}}{\left(K_{S1} + S_1^*\right)^2} \qquad a_2 = \frac{\mu_{2max}^* K_{S2}}{\left(K_{S2} + S_2^*\right)^2} \tag{12}$$

and matrix B is obtained as:

$$B = [B_w \,|B_u\,] = \left[\begin{array}{c|c} 0 & -X_1^* \\ 0 & -X_2^* \\ D & S_1^{in} - S_1^* \\ 0 & S_1^* - S_2^* \end{array}\right] \tag{13}$$

and matrix C is similarly obtained as:

$$C = \begin{bmatrix} 0 & k_4 \mu_2^* & 0 & a_2 k_4 X_2^* \end{bmatrix} \tag{14}$$

The state-space representation of the linearized system is presented as follows:

$$\begin{aligned} x\left(k+1\right) &= Ax\left(k\right) + B_u u\left(k\right) + B_w w\left(k\right) \\ y\left(k\right) &= Cx\left(k\right) + Du\left(k\right) \end{aligned} \tag{15}$$

The resulting model is an approximation of the dynamics of the nonlinear system around the equilibrium point defined. In order to understand the linearization process, the linearized model with its variables is depicted in Figure 1. Here, $w(k)$ and $u\left(k\right)$ are the disturbance and control inputs, respectively; $y(k)$ is the constrained output; and, finally, $z(k)$ is the performance output, which is the difference between the desired and actual outputs. As usual, the purpose of the control is to make the performance output reach the reference signal; in other words, the controller deals with a reference tracking problem. The MATLAB Simulink 'linmod' function is utilized when obtaining the state-space representation of the system, shown in Figure 1.

The moving horizon $\mathcal{H}_\infty$ control system developed is a full-state feedback control system. Since the states cannot be measured online for this process, a state observer is needed to be designed and integrated. It is clear that the system has to be fully observable. The state-space representation of such an observer is presented as follows:

$$\begin{aligned} \hat{x}\left(k+1\right) &= A\hat{x}\left(k\right) + B_u u\left(k\right) + B_w w\left(k\right) + L\left(y\left(k\right) - \hat{y}\left(k\right)\right) \\ \hat{y}\left(k\right) &= C_1 \hat{x}\left(k\right) + Du\left(k\right) \end{aligned} \tag{16}$$

where $\hat{x}\left(k\right)$ and $\hat{y}\left(k\right)$ denote the observed states and observed output, respectively. The difference between the dynamics of the real system $x(k+1)$ and the observed system $\hat{x}\left(k+1\right)$ constitutes the error dynamics $\hat{e}\left(k+1\right)$.

$$\hat{e}\left(k+1\right) = \left(A - LC\right) e\left(k\right) \tag{17}$$

As seen in Eq. (17), the error will converge to 0 depending on the eigenvalues of $\left(A - LC\right)$, which are determined by the elements of L.

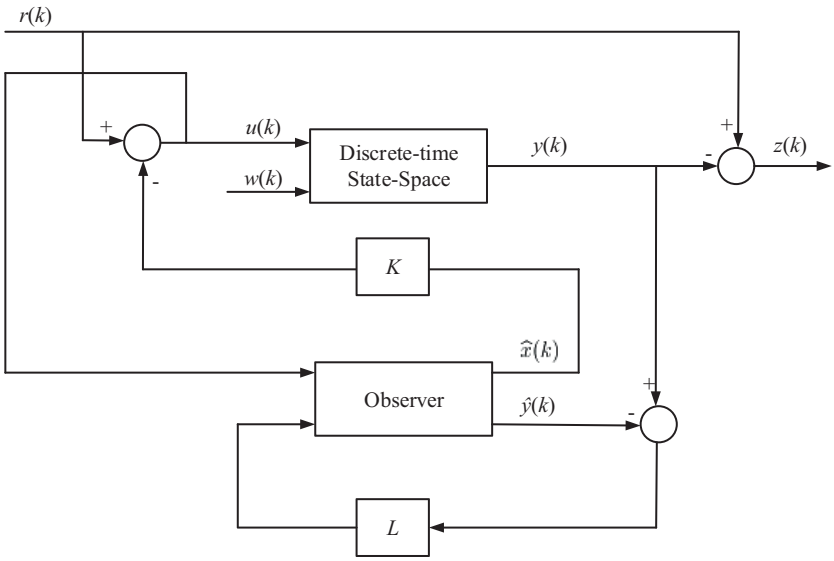

Figure 1. Linear state-space model (linmod) of the system with reference.

4. LMI-based moving horizon $\mathbf{H}_\infty$ control

The linear discrete-time system to be dealt with is represented by the following state equations:

$$x(k+1) = Ax(k) + B_u u(k) + B_w w(k)$$

$$\begin{aligned} z_1(k) &= C_1 x(k) + D_{1u} u(k) + D_{1w} w(k) \\ z_2(k) &= C_2 x(k) + D_{2u} u(k) \end{aligned} \tag{18}$$

where $x(k) \in R^n$ is the state vector and $u(k)\, w(k) \in R^m$ are the control input and disturbance vectors, respectively. The performance and constrained outputs are

$z_1(k)\, z_2(k) \in R_\cdot^P$

At each step k for $k > 0$, the optimization problem of the constrained $\mathcal{H}_\infty$ control is presented in Eq. (19) and the LMIs are given in Eqs. (20) through (23).

$$\min_{\gamma, L, Y, X} \gamma \tag{19}$$

$$\begin{bmatrix} Y & * & * & * \\ 0 & \gamma^I & * & * \\ AY + B_u L & B_w & Y & * \\ C_1 Y + D_{1u} L & D_{1w} & 0 & \gamma I \end{bmatrix} > 0 \tag{20}$$

$$\begin{bmatrix} \frac{1}{r} X & L \\ L^T & Y \end{bmatrix} \geq 0 \quad X_{ii} \leq u_{i,max}^2 \tag{21}$$

$$\begin{bmatrix} r - \gamma^2 a^2 & x(k)^T \\ x(k) & Y \end{bmatrix} \geq 0 \tag{22}$$

$$\begin{bmatrix} p_0 - p_{k-1} + x(k)^T P_{k-1} x(k) & x(k)^T \\ x(k) & Y \end{bmatrix} \geq 0 \tag{23}$$

Here, $Y = P^{-1}$, $L = KP^{-1}$, and p_0 and p_k are defined as follows:

$$p_0 = x(0)^T P_0 x(0),$$

$$p_k := p_{k-1} - \left[x(k)^T P_{k-1} x(k) - x(k)^T P_k x(k) \right]. \tag{24}$$

The terms γ_k, L_k, Y_k, X_k are obtained by solving Eq. (19) by means of the LMIs given in Eqs. (20) through (23) for each instant k. Thanks to the LMIs' terms, the control signal,

$$u(k) = K_k x(k) \tag{25}$$

is applied to the system while calculating the feedback gain $K_k = L_k Y_k^{-1}$ After updating the states, it is continued with the next step and the optimization problem is iterated. Since the actual state $x(k)$ exists in the liner matrix inequalities of Eqs. (22) and (23), the feedback gain K_k changes accordingly. The algorithm proposed and developed by Chen and Scherer in [7,8] is explained with a flowchart in Figure 2.

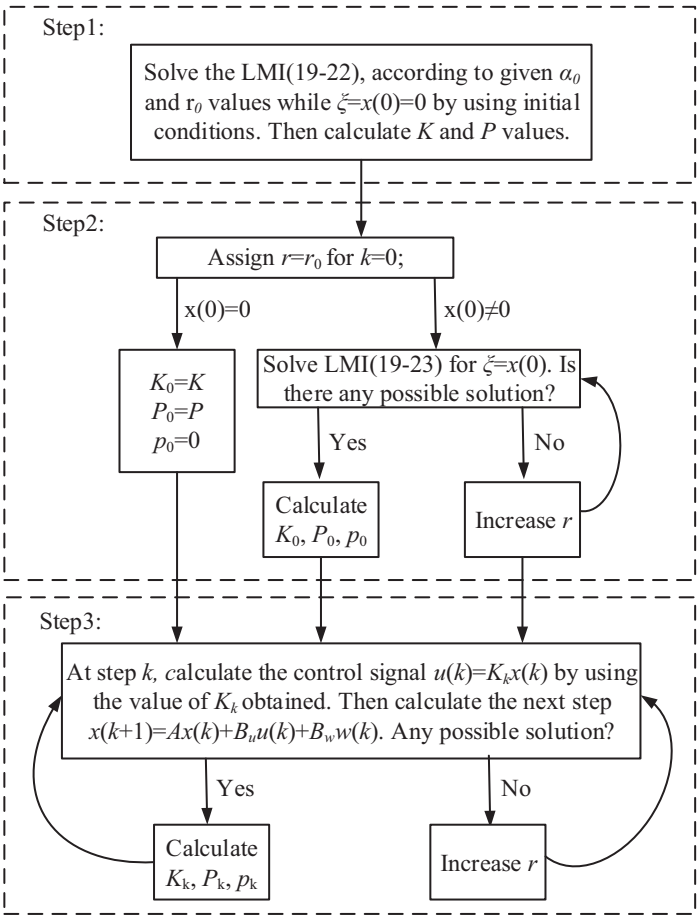

Figure 2. The flowchart of the algorithm for the moving horizon $\mathcal{H}_\infty$ control.

The LMIs given in Eqs. (20) to (23) used in the algorithm can be described briefly as follows. The LMI in Eq. (20) is used for the solution of the state feedback $\mathcal{H}_\infty$ control problem in Figure 3. While the stability of the closed-loop system obtained is guaranteed, the performance index from $w(k)$ to $z(k)$ is constrained by means of this LMI. This means the dissipativity condition below is met:

$$V\left(x\left(k+1\right)\right)-V\left(x\left(k\right)\right)+\left\|z\left(k\right)\right\|-\gamma^{2}\left\|w\left(k\right)\right\|<0 \tag{26}$$

There must be a $P>0$ matrix in the sense of the Lyapunov function, $V\left(x\left(k\right)\right)=x^{T}\left(k\right)Px\left(k\right)$ in order to meet the stability condition.

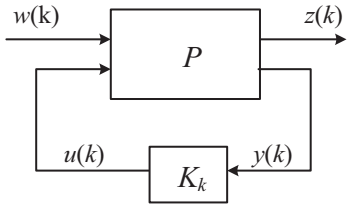

Figure 3. The block diagram for the $\mathcal{H}_\infty$ control problem.

On the other hand, in order to make the closed-loop system gain smaller than the gain γ, which is measured from the performance output to the disturbance input, as described in Eq. (27):

$$\frac{\left\|z\left(k\right)\right\|_{2}}{\left\|w\left(k\right)\right\|_{2}}<\gamma^{2} \tag{27}$$

the closed-loop system takes the following form by means of the feedback rule, $u=Kx$.

$$\begin{aligned} x\left(k+1\right)&=A_{cl}x\left(k\right)+B_{w}w\left(k\right)\\ z_{1}\left(k\right)&=C_{cl}x\left(k\right)+D_{w}w\left(k\right)\end{aligned} \tag{28}$$

Here, $A_{cl}=A+B_{u}K$ and $C_{cl}=C+D_{u}K$.

Hence, in order to create the $\mathcal{H}_\infty$ control LMI, the dissipativity inequality in Eq. (26) and the closed-loop system of Eq. (28) can be represented in matrix form as follows:

$$\begin{bmatrix} x\left(k\right)\\ w\left(k\right)\end{bmatrix}^{T}\begin{bmatrix} A_{cl}^{T}PA_{cl}-P+C_{cl}^{T}C_{cl} & A_{cl}^{T}PB_{w}+C_{cl}^{T}D_{w}\\ * & B_{w}^{T}PB_{w}+D_{w}^{T}D_{w}-\gamma^{2}I\end{bmatrix}\begin{bmatrix} x\left(k\right)\\ w\left(k\right)\end{bmatrix}<0 \tag{29}$$

where the square matrix must be negative in order to meet the inequality in Eq. (29). If the Schur complement formula is applied:

$$\begin{bmatrix} -P^{-1} & 0 & P^{-1}A_{cl}^{T} & P^{-1}C_{cl}^{T}\\ * & -\gamma^{2}I & B_{w}^{T} & D_{w}\\ * & * & -P^{-1} & 0\\ * & * & * & -I\end{bmatrix}<0 \tag{30}$$

and A_{cl} and C_{cl} are substituted, the inequality in Eq. (31) is obtained as follows:

$$\begin{bmatrix} Y & 0 & YA^T + L^T B_u^T & YC^T + D_{1u}^T L^T \\ * & \gamma I & B_w^T & D_w \\ * & * & Y & 0 \\ * & * & * & \gamma I \end{bmatrix} \tag{31}$$

The LMI in Eq. (21) shows the constraint $\|u(k)\|_{\max} = u_{i,max}^2$, which bounds the energy of the control input $u(k) = LY^{-1}x(k)$. In this case, the LMI in Eq. (21) is obtained as follows:

$$|u_i(k)|^2 = \left|\left(LY^{-1}\right)_i x(k)\right|^2 \tag{32}$$

The state constraint, which forces the states to remain within an ellipsoid, is shown in Eq. (33):

$$\varepsilon_1(P, r) := \{x \in R^n : V(x) \leq r\} \tag{33}$$

In this case, the constraints become the following:

$$\begin{aligned} \|u(k)\|_{\max} &\leq \left|\left(LY^{-1}\right)_i x\right|^2, \\ &\leq r\left\|\left(LY^{-1}\right)_i\right\|_2^2. \end{aligned} \tag{34}$$

The inequality in Eq. (34) becomes Eq. (35) after the application of the Schur complement, as follows:

$$\begin{bmatrix} \frac{1}{r}X & L \\ L^T & Y \end{bmatrix} \geq 0 \quad X_{ii} \leq u_{i,max}^2 \tag{35}$$

supposing the energy of the disturbance is constrained as:

$$\sum_{i=0}^{\infty} \|w(i)\|^2 \leq \|\alpha\|^2 \tag{36}$$

The initial state $x(0)$ should be guaranteed to be contained in the ellipsoid ε_2, which is defined as:

$$\varepsilon_2(P, r, \alpha) := \left\{x \in R^n \ : \gamma^2\alpha^2 + V(x) \leq r\right\} \tag{37}$$

The LMI in Eq. (22) is the Schur complement of the inequality in Eq. (37), which guarantees the disturbance to be bounded and is given in Eq. (38).

$$\begin{bmatrix} r - \gamma^2\alpha^2 & \xi(k)^T \\ \xi(k) & Y \end{bmatrix} \geq 0 \tag{38}$$

On the other hand, the LMI defined in Eq. (23) is required to meet the dissipation constraint condition online. If the Schur complement formula is applied for this LMI, the following is obtained as:

$$p_{0-}p_{k-1} + x(k)^T P_{k-1} x(k) - x(k)^T P_k x(k) \geq 0 \tag{39}$$

where $p(0)$ and $p(k)$ are computed recursively, as given in Eq. (21). Detailed information on how to obtain and prove this constraint can be found in [9].

5. Experimental results

This section presents the results of the simulation experiments obtained with the application of three different control approaches to the mathematical model of an anaerobic wastewater system. The parameters of the anaerobic system to be controlled are presented in Table 1. The values at the operating points, where the linearization process is performed, are selected as $D = 0.03\,(day^{-1})$ and $S_1^{in} = 1\,(g/l)$.

Table 1. Parameters of anaerobic system [13].

$\mu_{1max}\ (day)^{-1}$	$\mu_{2max}\ (day)^{-1}$	$K_{s1}\ (g/L)$	$K_{s2}\ (g/L)$	k_1	k_2	k_3	k_4
0.2	0.25	0.3	0.87	6.7	4.2	5	4.35

The system is linearized with these values and sampled with a sampling time of $T = 0.1s$. The matrices required for the system being used for reference tracking are presented below.

$$A = \begin{bmatrix} 0.9999 & 0 & 0.0066 & 0 \\ 0 & 1 & 0 & 0.0023 \\ -0.0196 & 0 & 0.9525 & 0 \\ 0.0122 & -0.0149 & 0.0307 & 0.9853 \end{bmatrix}$$

$$B_w = \begin{bmatrix} 0 & 0 \\ 0 & 0 \\ 0 & 0.0029 \\ 0 & 0 \end{bmatrix} \qquad B_u = \begin{bmatrix} -0.0138 \\ -0.0106 \\ 0.0926 \\ -0.0051 \end{bmatrix}$$

$$C_y = \begin{bmatrix} 0 & 0.132 & 0 & 1.79 \end{bmatrix} \qquad C_z = \begin{bmatrix} 0 & -0.132 & 0 & -1.79 \end{bmatrix}$$

As explained with the flow diagram presented in Figure 2, first, the minimum γ_{opt} is computed for the H_∞ problem with no constraint. Next, γ_{opt}= 1.2247 is found for this problem. The parameter for bounding the disturbance is selected as $\alpha = 1$ and consequently r_0= $10\gamma_{opt}^2\alpha^2$ is obtained. In this case, the control input is constrained as $\|u\,(k)\|_{\max} \leq 10$.

During the control experiments, first, the PID controller is applied to the system, which is linearized and controlled with the parameters presented previously. The PID coefficients that make the controller performance optimum are obtained by means of the Ziegler–Nichols method and given in Table 2. A step function representing a typical disturbance input, as shown in Figure 4a, is applied to the system controlled with the PID controller. The behavior of the states of the system during the control is presented in Figure 4b. The control signal that is responsible for the changes in the states is plotted in Figure 4c. It is practically introduced by the input valve, which manipulates the dilution rate (D). Due to the effect of the integral term of the PID controller, the CH_4 gas output reaches the desired level in a reasonably short time, as seen in Figure 4d. However, it should be noted that the PID coefficients computed are valid only for the operating point taken into consideration.

Table 2. PID coefficients computed by means of the Ziegler–Nichols method.

K_P	K_I	K_D
2.23	0.98	1.32

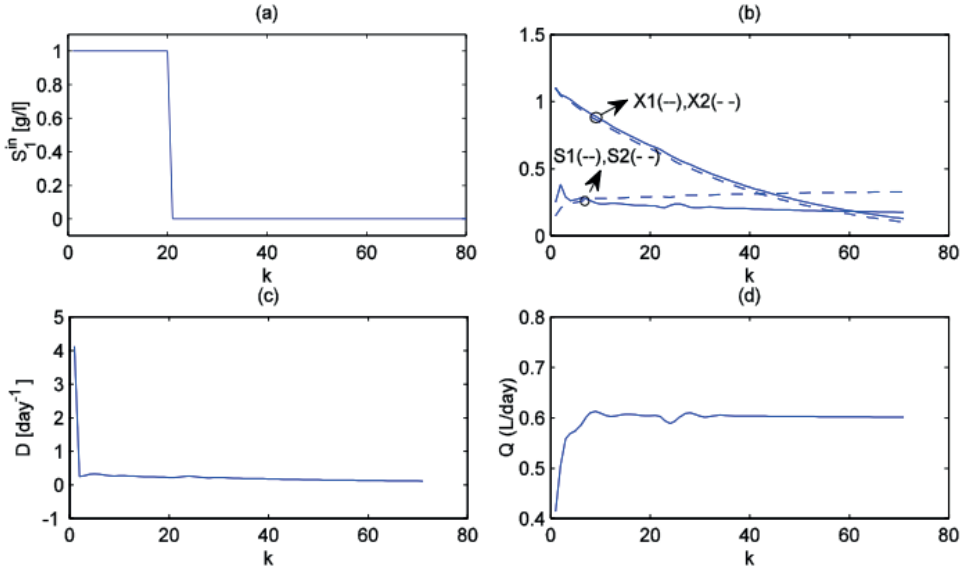

Figure 4. PID control of the anaerobic system: a) disturbance $w(k)$; b) bacteria growth curves in the reactors (X_1X_2) and substrate levels (S_1S_2) ; c) control input, $u(k)$; d) CH_4 gas output $y(k)$.

Next, in the second step, the system of interest is controlled first with the classical $\mathcal{H}_\infty$ controller followed by the moving horizon $\mathcal{H}_\infty$ controller. The simulation results obtained from these two control approaches are plotted in the same graph, as presented in Figure 5. The same disturbance was introduced to the system. The changes in the state variables of the first and the second reactor are shown in Figure 5a and Figure 5b, respectively. The energy of control signals is presented in Figure 5c and the CH_4 gas outputs in Figure 5d. The CH_4 gas outputs produced by applying the moving horizon $\mathcal{H}_\infty$ and classical $\mathcal{H}_\infty$ controls to the system are plotted in the same graph for comparison, as seen in Figure 5d. In the moving horizon $\mathcal{H}_\infty$ control method, since the constraints can be included in the system and the system gain γ can also be optimized with respect to the disturbance at every step, and the input signal can then be recomputed accordingly, better results are observed. Furthermore, the energy of the control signal used for the moving horizon control is smaller compared to the other controls employed, as clearly indicated by Figure 5d.

6. Conclusions

Anaerobic wastewater treatment systems involve high degrees of nonlinearities and uncertainties. They are also exposed to large-scale disturbances. In this study, such an anaerobic system was first represented with a nonlinear mathematical model that could be found in the literature. The system parameters were selected based on real laboratory experiments carried out previously and also from the reported research works. The model was then linearized for the operating points and discretized with a sampling period of 0.1 sec. The system was controlled first with a conventional PID controller to provide a kind of validation base for the following experiments. Next a classical $\mathcal{H}_\infty$ controller and finally a moving horizon $\mathcal{H}_\infty$ controller were developed and applied to obtain flexible control strategies to deal with bounded disturbances and control inputs. After summarizing the whole work accomplished within the framework of this paper, the concluding remarks can be derived as follows.

As stated earlier, when it is desired to make changes in parameters or constraints, or alternatively to work in different operating points for different wastewaters, $\mathcal{H}_\infty$ control and moving horizon $\mathcal{H}_\infty$ control prove

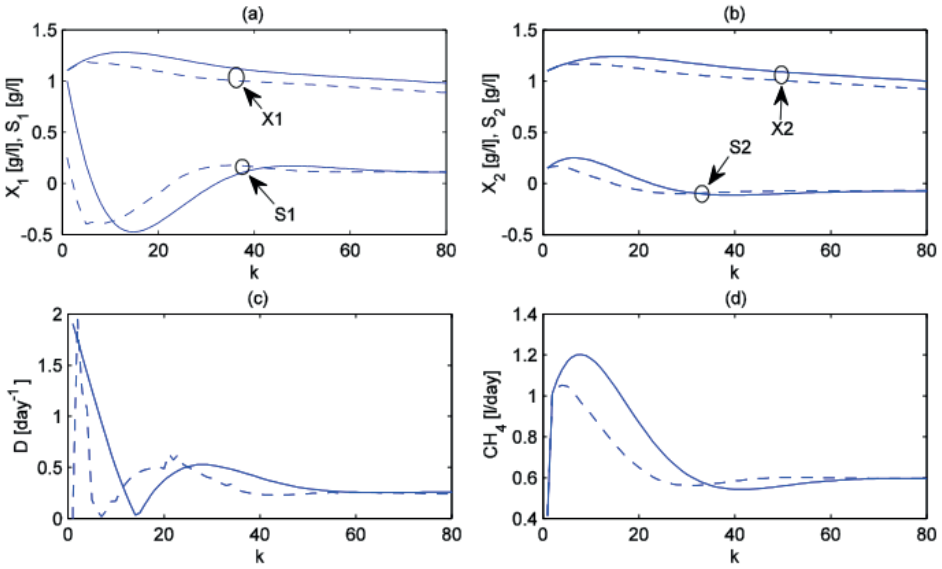

Figure 5. Moving horizon $\mathcal{H}_\infty$ control ($--$) vs. $\mathcal{H}_\infty$ control (—) on: a) state variables of the first reactor; b) state variables of the second reactor; c) energy of inputs $\|u(k)\|$; d) controlled outputs, $z(k)$.

themselves as more versatile methods, whereas if worked with a PID controller, the coefficients have to be recalculated offline for each case, which brings a computational workload and is difficult to implement.

As can be appreciated from the experiments and simulation results, the moving horizon $\mathcal{H}_\infty$ controller allows the control constraints to be introduced and conformed while providing the stability of the closed-loop system. However, there is still a trade-off between complying with the constraints and the performance. The operator needs to make compromises in the performance in order to guarantee the stability while remaining within the bounds.

As a future work, the observer structure integrated with the controller will be improved further to obtain better approaches to the unmeasurable parameters of the system. In fact, this would be a great contribution, since mathematical models developed for such processes have a deficit of reachable parameters. Better control performances can be expected in this way. Another future work would be the evaluation of the performance of the controller under different operating conditions when the system involves a time delay. Consequently, remedies to overcome the delay problem could be studied. Additionally, as a sequential work, the simulation results obtained will be reevaluated on the basis of the experimental results obtained from a pilot-scale anaerobic reactor, which was constructed within a project supported by the Scientific and Technological Research Council of Turkey (TÜBİTAK).

References

[1] Mayne DQ, Rawlings JB, Rao CV, Scokaert POM. Constrained model predictive control: Stability and optimality. Automatica 2000; 36: 789–814.

[2] Qin SJ, Badgwell TA. A survey of industrial model predictive control technology. Control Eng Pract 2003; 11: 733–764.

[3] Camacho E, Bordons C. Model Predictive Control. Berlin, Germany: Springer-Verlag, 2004.

[4] Michalska H, Mayne DQ. Robust receding horizon control of constrained nonlinear systems. IEEE T Automat Contr 1993; 38: 1623–1633.

[5] Kwon WH, Han S. Receding Horizon Control. Berlin, Germany: Springer-Verlag, 2005.

[6] Kothare MV, Balakrishnan V, Morari M. Robust constrained model predictive control using linear matrix inequalities. Automatica 1996; 32: 1361–1379.

[7] Chen H, Scherer C. Moving horizon control with performance adaptation for constrained linear systems. Automatica 2006; 42: 1033–1040.

[8] Chen H, Scherer C. Disturbance attenuation with actuator constraints by moving horizon control. In: 2003 International Federation of Automatic Control Symposium on Advanced Control of Chemical Processes; Hong Kong. pp. 447–452.

[9] Chen H, Gao XQ, Wang H. On disturbance attenuation of nonlinear moving horizon control. Lect Notes Contr Inf 2007; 358: 283–294.

[10] Holenda B, Domokos E, Redey A, Fazakas J. Dissolved oxygen control of the activated sludge wastewater treatment process using model predictive control. Comput Chem Eng 2008; 32: 1270–1278.

[11] Shen W, Chen X, Pons MN, Corriou JP. Model predictive control for wastewater treatment process with feedforward compensation. Chem Eng J 2009; 155: 161–174.

[12] Taşçıkaraoglu, F. Y., Ucun, L., & Küçükdemiral, I. B. Receding horizon $\mathcal{H}_\infty$ control of time-delay systems. Transactions of the Institute of Measurement and Control 2014; DOI: 10.1177/0142331214538089.

[13] Simeonov I, Queinnec I. Linearizing control of the anaerobic digestion with addition of acetate (control of the anaerobic digestion). Control Eng Pract 2006; 14: 799–810.